Anomalous ground states at the interface between two transition-metal compounds

Michel van Veenendaal*
Department of Physics, Northern Illinois University, De Kalb, Illinois 60115, USA
and Advanced Photon Source, Argonne National Laboratory, 9700 S. Cass Avenue, Argonne, Illinois 60439, USA
(Received 25 March 2008; revised manuscript received 22 September 2008; published 16 October 2008)

The effects of strong covalency across a strongly correlated interface between two transition-metal compounds are studied. Since the charge transfer is directional, the lowest electron-removal and -addition states are often not involved in the formation of covalent bonds across the interface. This paper shows that this can lead to the formation of unusual ground states not found in the bulk. For cuprates, the formation of "Zhang-Rice triplets" is observed. For nickelates, we demonstrate the possibility of in-plane or out-of-plane orbital switching, whereas cobaltates are prone to spin switching. For Co and Fe compounds, a change between antiferromagnetic superexchange and ferromagnetic double exchange is found. Calculations of x-ray magnetic dichroism are presented, which could provide insight into the presence of these unusual ground states.

DOI: 10.1103/PhysRevB.78.165415 PACS number(s): 73.20.−r, 71.27.+a

I. INTRODUCTION

In recent years, the study of the interfacial behavior of transition-metal compounds has led to several surprising discoveries, including the presence of metallic behavior at the interface of Mott and band insulators[1–3] and tunable quasi-two-dimensional electron gases.[4] These phenomena are often related to charge transfer at the interface. For example, charge transfer from a $3d^1$ Mott insulator to a $3d^0$ band insulator can effectively dope both sides of the interface and can lead to metallic behavior.[1] Also, electron dissipation from $CaRuO_3$ into the antiferromagnetic insulator $CaMnO_3$ can lead to ferromagnetism in the layer adjacent to the interface through the double exchange mechanism.[5] These phenomena can be understood on the basis of effective electron and hole doping of the interfacial layers and do not directly depend on a reconstruction of the electronic structure. However, to facilitate the exchange of charge across the interface, the electronic structure can also be modified by the formation of covalent bonds. Recently, an orbital reconstruction was demonstrated experimentally at a cuprate/manganite interface.[6] In this paper, the general trends in local orbital and spin structure of late transition-metal compounds close the interface are described, and the consequences of orbital recontruction due to strong covalency are discussed. Crucial for the understanding of the local electronic structure at the interface is that the bulk quasiparticles have often zero spectral weight when electrons are added or removed through the ligands connecting the two materials. This has as a result that the lowest electron-addition and -removal states are not involved in the charge-transfer processes, leading to ground states that are counterintuitive to what one would expect from the bulk properties. For example, it is shown that the surface can sustain a considerable amount of "Zhang-Rice triplets," contrasting the bulk, where the low-energy physics is solely determined by Zhang-Rice singlets.[7] The charge transfer across the interface can be varied by changing the compounds, the doping levels, and the strain or by applying an external potential across the interface. It is shown that, when tuning the interfaces, small changes in charge transfer can lead to drastic changes in ground state properties. This distinct switching between different states greatly enhances the possibility for technological applications. Predicted effects include orbital switching with a sudden change from out-of-plane to in-plane charge density, spin switching between intermediate and low-spin phases, and the possibility to change the magnetic coupling across the interface from ferromagnetic to antiferromagnetic.

Trends of local spin and orbital structures at interfaces of transition-metal compounds are often difficult to study. Density-functional theory (DFT) (Refs. 5, 8, and 9) includes the necessary detail but would require many complex calculations to obtain a variation in the work function. On the other hand, many-body techniques using exact diagonalization[10] and dynamical mean-field theory[1] often use strongly simplified Hamiltonians that fail to describe the detailed orbital and spin transitions. In order to obtain a general understanding of the local spin and orbital character of the ions adjacent to the interface, cluster calculations were employed. These calculations have the advantage of exactly diagonalizing the Coulomb interactions, including the higher-order terms (leading to the Hund's coupling) while maintaining sufficient material-specific details. We assume that the excess charge decreases exponentially[5] and that the change in local electronic and magnetic structure occurs predominantly in the transition-metal layer adjacent to the interface as was observed experimentally.[6] The goal of the paper is to describe phenomena that can occur at the interface of transition-metal compounds. Several possible unusual ground states will be identified. The paper hopes to stimulate further experimental and theoretical work to demonstrate the existence of these states in more realistic systems.

The paper is divided as follows. The theoretical methods are described. The local hole densities and symmetries of transition-metal ions adjacent to an interface are discussed for copper, nickel, cobalt, and iron. Since interfaces cannot be studied with surface-sensitive techniques, such as photoemission, calculations of x-ray absorption and dichroism are presented. X-ray absorption spectroscopy (XAS) and x-ray magnetic dichroism (XMD) are sensitive to changes in the local ground state symmetry. The paper ends with a discussion.

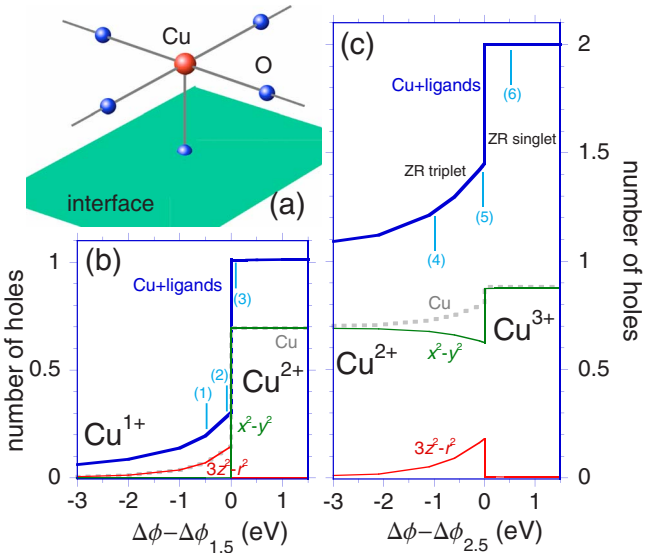

FIG. 1. (Color online) Hole densities on interfacial Cu as a function of the difference in work function. (a) A CuO_5 cluster connected to an interface. The assumption is made that the electronic states at the other side of the interface function as a reservoir of holes and electrons that couples to the e_g states. The work-function difference between copper and the reservoir is given by $\Delta\phi$. (b) The hole densities in $3d_{x^2-y^2}$ (green), $3d_{3z^2-r^2}$ (red), on Cu total (gray dotted), and on Cu and ligand (blue) on the CuO_5 cluster adjacent to the interface. The value $\Delta\phi_{1.5}$ for which copper has a formal valency of 1.5+ has been subtracted. The numbers indicate the values for which x-ray absorption spectra have been calculated (see Fig. 3). (c) Idem, but now the valency is changing from 2+ to 3+ (the value of $\Delta\phi$ for $Cu^{2.5+}$ has been subtracted).

II. THEORY

The numerical calculations of the hole density and the L-edge x-ray absorption spectra were based on a cluster consisting of a transition-metal ion and a sixfold (fivefold for copper compounds) surrounding of ligands. The Hamiltonian includes a one-particle part consisting of on-site energies, crystal-field parameters (1 eV for Ni, Co, and Fe), spin-orbit parameters,[11] hopping parameters (with $pd\sigma=1.5$ eV for Cu and 1.3 eV for Ni, Co, and Fe compounds[12–14]), and a many-body part consisting of the $3d$-$3d$ and $2p$-$3d$ Coulomb interactions. Parameters used in the calculations are based on those for oxides.[12–14] The monopole part of the Coulomb interactions is taken as 6 eV. Off-diagonal Coulomb matrix elements were calculated in the Hartree-Fock limit and scaled down to 80% to account for screening effects.[11,15] The charge-transfer energies are defined as

$$\Delta = E_{\text{low}}(3d^{n+1}\underline{L}) - E_{\text{low}}(3d^n), \tag{1}$$

where $\underline{L}$ stands for a hole on the ligands and E_{low} is the lowest energy for a particular configuration. Therefore, Δ is the lowest energy to transfer an electron from the ligands to the transition-metal site. The values are $\Delta=2.2,5,4,5$ eV for Cu^{2+}, Ni^{2+}, Co^{2+}, and Fe^{2+} ($n=9$, 8, 7, and 6), respectively. In the apical direction, the ligand is coupled to $3d$ states at the other side of the interface [see Fig. 1(a)]. To obtain the trends of the influence of the interface on the local ground state, we take the other side of the interface basically as a reservoir of electrons or holes in a way similar to the method used in Ref. 16. The assumption is that the coupling across the interface is dominated by the states close to the Fermi level. The energy position is determined by the difference in work function between the compounds, which can depend on the material, the doping level, lattice relaxation, etc. To keep the size of the calculation under control, the bandwidth of this reservoir is neglected. The reservoir states are taken to be spin polarized by taking an exchange splitting of 2 eV on the spin of the reservoir states. The spin-up density of states (DOS) is assumed to be full. This allows the study of the magnetic coupling across the interface. Trends in interfacial ground states are obtained by treating the difference in work functions $\Delta\phi$ as an adjustable parameter allowing a continuous change in the charge transfer across the interface.

X-ray aborption spectra are calculated using Fermi's golden rule

$$I_q(\omega) = \sum_f |\langle f|D_q|g\rangle|^2 \delta(\hbar\omega + E_g - E_f), \tag{2}$$

where $\hbar\omega$ is the energy of the incoming photon and $|g\rangle$ and $|f\rangle$ are the ground and final states, respectively; D_q is the dipole transition operator for a particular polarization q. The three polarization directions are combined to give the isotropic $(I_1+I_0+I_{-1})$, the circular dichroic (I_1-I_{-1}), and the linear dichroic $(I_1-2I_0+I_{-1})$ spectra. Note that, in antiferromagnetic systems, the circular dichroic spectra from different sites will cancel.

III. COPPER COMPOUNDS

Let us first consider the situation of a copper ion adjacent to an interface. Divalent copper compounds, such as CuO and undoped high-T_c cuprates, have a $3d^9$ configuration. This state is unstable to Jahn-Teller distortions[17] that split the x^2-y^2 and $3z^2-r^2$ orbitals. In a local D_{4h} symmetry the hole density is in the x^2-y^2 orbital. The charge transfer is relatively small, about 2–3 eV, compared to other late transition-metal compounds. This makes the ground state covalent with about 0.7 holes on copper and 0.3 holes on the surrounding ligands.[18]

For the situation where electron density is transferred to the cuprate, see Fig. 1(a), one expects the remaining hole density to reside in the $3d_{x^2-y^2}$ orbitals, which are known to dominate the electronic structure in the bulk[7,14] and are often the only orbitals included in model Hamiltonians. Surprisingly, when electrons are transferred, the remaining hole density is in the $3d_{3z^2-r^2}$ orbital, see points (1) and (2) in Fig. 1(b), as was recently found experimentally.[6] The underlying physics can be understood by the formation of a covalent bond between copper and the transition-metal states at the other side of the interface via the connecting ligand at the interface. This bond formation only occurs with the out-of-plane $3d_{3z^2-r^2}$ orbital since the hopping integral between the in-plane $3d_{x^2-y^2}$ orbital and the apical ligand is zero. This covalent bond formation gives rise to a magnetic coupling across the interface [see Figs. 2(a) and 2(b)]. The sign of the

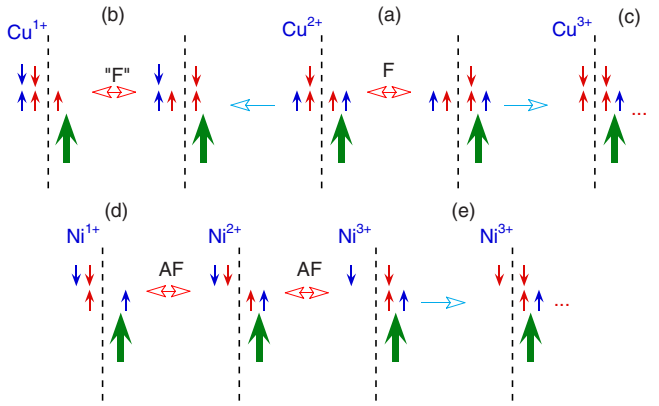

FIG. 2. (Color online) Schematic figure of the dominant charge fluctuations across the interface (indicated by the dashed line). The small red and blue arrows indicate electrons in the x^2-y^2 and $3z^2-r^2$ orbitals, respectively. The large green arrow denotes a core spin leading to a spin polarization of the e_g electrons in the reservoir. The blue arrows indicate that a change in symmetry has occurred and that different charge fluctuations now dominate. (a) A Cu^{2+} ion ($3d^9$) coupled to a compound where the spin-up DOS is occupied leading to ferromagnetic fluctuations inducing Zhang-Rice triplet character on the Cu side. This corresponds to points (3)–(5) in Fig. 1. (b) An electron is transferred to the copper giving Cu^{1+} [$3d^{10}$, points (1) and (2)] with ferromagnetic fluctuations. (c) An electron is transferred to the reservoir creating Zhang-Rice singlets on the copper side [point (6) in Fig. 1]. Charge fluctuations are strongly suppressed. (d) Charge fluctuations starting from a Ni^{2+} ion [points (1)–(10) in Fig. 4]. Note that there is no change in symmetry in going from Ni^{2+} to Ni^{1+}. (e) Orbital reconstruction changing the hole density from out of plane to in plane [points (11) and (12) in Fig. 4]. Charge fluctuations are reduced.

coupling depends on the type of ions on the opposite site of the interface and follows the usual Goodenough-Kanamori rules.[17,19] In the calculations, we assume an electron density in the e_g orbitals to allow the possibility of electron and hole doping. We also take a core spin into account. This represents the t_{2g} electrons and fixes the magnetic direction. An electron from $3z^2-r^2$ couples to the empty $3z^2-r^2$ DOS. In this case, the empty DOS is antiparallel to the core spins, and the induced spin on the copper aligns parallel to the core spins in the reservoir [see Fig. 2(b)]. On the other hand, in the case of a cuprate coupled to doped manganites studied by Chakhalian *et al.*,[20] there will be empty spin-up density of states close to the Fermi level, causing the induced spin on copper to be antiparallel to the manganese spins. This situation was also studied giving a change in hole density comparable to that in Fig. 1(a) (not shown).

Upon further increasing the hole density on the copper, the covalent state becomes energetically unfavorable with respect to the in-plane $3d_{x^2-y^2}$ states, which is the typical configuration found for divalent copper compounds. The covalent-to-in-plane bond transition is sudden and accompanied by an increase in the number of holes on the CuO_5 cluster from 0.3 to 1. The magnetic coupling across the interface is due to the delocalization of the electron in the $3d_{3z^2-r^2}$ orbitals. However, no charge can flow onto the copper site since both $3d_{3z^2-r^2}$ orbitals are filled [see Fig. 2(a)].

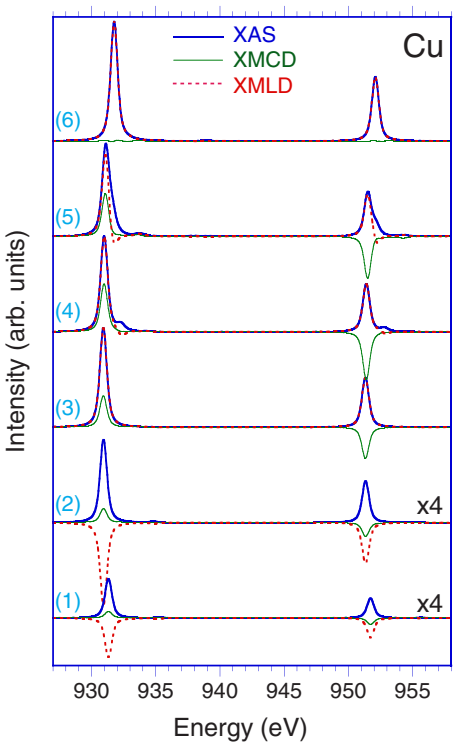

FIG. 3. (Color online) Cu L-edge x-ray absorption (blue), x-ray magnetic circular dichroism (thin green), and x-ray magnetic linear dichroism spectra (dotted red) for the values of the difference in work function given in Fig. 1.

The coupling therefore is a result of the delocalization of $3d_{3z^2-r^2}$ electron from copper into the reservoir. Since we have taken the spin-up states to be full, the electron couples antiparallel to the core spin, causing an antiferromagnetic superexchange coupling. After the transition, the $3d_{x^2-y^2}$ orbital is filled with an electron from a $3d_{x^2-y^2}$ in the reservoir. Since the $3z^2-r^2$ density of states in the reservoir is full, $3d_{3z^2-r^2}$ from copper delocalizes in density of states antiparallel to the copper. Again, this leads to an antiferromagnetic exchange. The difference between the two configurations can be demonstrated using x-ray magnetic linear dichroism (XMLD) (see Fig. 3). The XMLD changes sign when the hole density moves from the $3z^2-r^2$ orbital to the x^2-y^2 orbital; see spectra (2) and (3) in Fig. 3.

Let us now consider the alternative situation where the cuprate is hole doped. Such a case was found theoretically using LDA+U calculations for $YBa_2Cu_3O_6/SrTiO_3$ heterostructures.[9] For large transferred hole densities, copper becomes formally trivalent (where by "formally" we imply the hole density on copper and its surrounding ligands), and one observes the formation of Zhang-Rice singlets (total spin $S=0$),[7,9,14] see point (6) in Fig. 1(c), with predominantly $\underline{3d_{x^2-y^2}}\underline{L}_{x^2-y^2}$ character (local symmetry $^1A_1$ in D_{4h}), where the underline indicates a hole and $\underline{L}_{x^2-y^2}$ stands for a hole on the ligands with x^2-y^2 symmetry. Unusual ground states are formed when fewer holes are transferred. The increased hole density is then in the covalent bond stretching across the interface; see points (4) and (5) in Fig. 1(c). The additional hole density does not form Zhang-Rice singlets, but are of a

triplet nature ($^3B_1$) with an orbital character of $\underline{3d}_{x^2-y^2}$ with $\underline{3d}_{3z^2-r^2}$ hole density mixed in. Note that the $3d_{x^2-y^2}$ hole density actually decreases with the holes pushed onto the ligands. The cuprate allows for an increase in formal valency of up to 2.5+ in Zhang-Rice triplet states before a discrete transition occurs into a Zhang-Rice singlet (formally Cu^{3+}). The presence of Zhang-Rice triplet character can be demonstrated using XMLD; see spectra (4) and (5) in Fig. 3. A clear difference is observed on the high-energy side of the XMLD spectra for Zhang-Rice triplet compared to Zhang-Rice singlets, where the XMLD is virtually identical to the XAS; see spectrum (6) in Fig. 3.

Summarizing, it is possible to both electron and hole dope cuprates by interfacing it with manganites[6] and early transition-metal oxides, respectively.[9] Essential for the local orbital and spin transitions is a critical hole and electron doping on the copper-oxygen units close to the interface. One can achieve this by interfacing the copper compound with materials with different work functions, thereby influencing the charge transfer across the interface. On the other hand, one can also change the doping level of the cuprate to bring the doping in the interfacial layer closer to the critical doping level. In addition, the transition could be affected by applying strain or an external potential.

IV. NICKEL COMPOUNDS

Divalent nickel is generally in a high-spin $\underline{3d}^2_{e_g}$ ($S=1$) state. NiO has an insulating gap of more than 4 eV,[21] which is significantly larger than that expected from band-structure calculations.[22] The electron-addition state is clearly $3d^9$ (^2E is O_h symmetry, i.e., a hole in the e_g states). The lowest electron-removal state has been more contentious. In their interpretation of x-ray photoemission data, Fujimori and Minami[23] suggested that the lowest electron-removal state is high spin ($^4T_1$ and comparable to the ground state of divalent cobalt). More recent cluster calculations using a better treatment of the covalency[12] indicate that the ground is more likely to be ^2E. Here the additional hole density is predominantly on the σ bonding ligands and couples antiparallel to the $S=1$ spin on nickel. Interpretation of L-edge x-ray absorption on doped nickel compounds[16] clearly favors the latter interpretation.

When bringing a nickel compound that is divalent in the bulk into contact with a system that donates e_g electrons, a covalent $3d_{3z^2-r^2}$-O_{p_z}-$3d_{3z^2-r^2}$ orbital is formed across the interface. When changing the work-function difference $\Delta\phi$, the electron density smoothly shifts between the different sides of the interface and no orbital reconstruction is observed; see points (1) and (3) in Fig. 4(a). For Ni^{1+}, the hole is in the $3d_{x^2-y^2}$ orbital, which is comparable to divalent copper. In addition, there is also no change in the magnetic coupling [see Fig. 2(d)]. Note that the magnetic coupling is opposite to that in the copper compounds. The transfer of electron density to the nickel ions adjacent to the surface creates empty spin-up density of states close to the Fermi level. Obviously, in real materials the sign of the magnetic coupling will depend on the interfacial compound. The change in

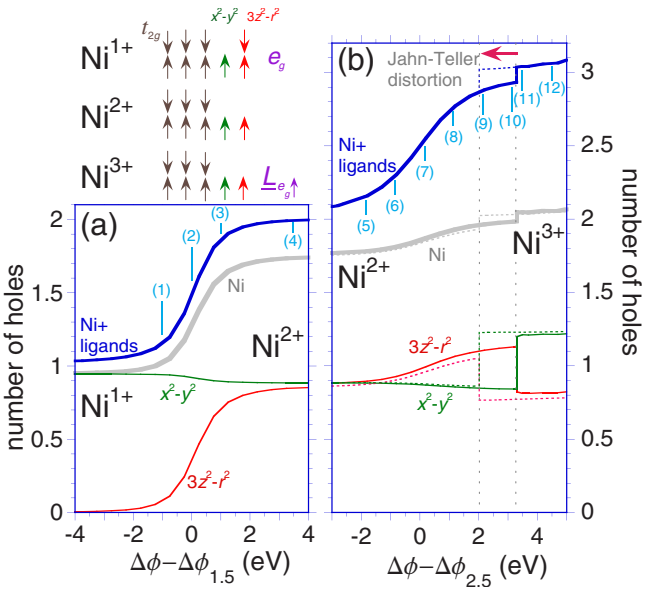

FIG. 4. (Color online) Hole densities on interfacial Ni as a function of the difference in work function. (a) The hole densities in $3d_{x^2-y^2}$ (green), $3d_{3z^2-r^2}$ (red), on Ni total (gray), and on Ni and the surrounding ligands (blue) on the NiO_6 cluster adjacent to the interface as a function of the work function difference $\Delta\phi$ between the nickel compound and the reservoir. In the case when the formal Ni valency changes from 1+ to 2+, the value $\Delta\phi_{1.5}$ for which nickel has a formal valency of 1.5+ has been subtracted. The numbers indicate the values for which x-ray absorption spectra have been calculated [see Fig. 5]. (b) Idem, but now the valency is changing from 2+ to 3+. The dotted lines show the values for the same calculation but now with a Jahn-Teller splitting of the e_g orbitals (the value of $\Delta\phi$ for $Ni^{2.5+}$ has been subtracted).

ground state densities can also be clearly observed in the x-ray absorption spectra; see spectra (1)–(5) in Fig. 5. The XAS develops from two white lines for Ni^{1+}, see spectrum (1), into a typical XAS spectrum for a divalent nickel oxide.[24] Note that there is a significant reduction in the XMLD signal related to the change from the planar x^2-y^2 hole density for Ni^{1+}, spectrum (1), to the more spherical $x^2-y^2, 3z^2-r^2$ hole density for Ni^{2+} [spectra (4) and (5)].

For the situation where electrons are removed from nickel, the additional holes couple antiparallel to the nickel moment[13] giving a predominantly $\underline{3d}_{3z^2-r^2\downarrow}\underline{3d}_{x^2-y^2\downarrow}\underline{L}_{e_g\uparrow}$ ground state; see inset in Fig. 4. However, at the interface the lower symmetry lifts the degeneracy of the e_g orbitals. The $3d_{3z^2-r^2}$ orbital forms a covalent bond across the interface, which is responsible for the initial increase in hole density when going from formally divalent to trivalent Ni; see points (6) to (10) in Fig. 4(b). However, for a planar nickel compound, one expects the hole density to be in the plane and not in the apical orbitals. Therefore, when the hole density is further increased, the system undergoes an orbital reconstruction in which the excess hole density changes from predominantly $\underline{3d}_{3z^2-r^2\downarrow}\underline{3d}_{x^2-y^2\downarrow}\underline{L}_{3z^2-r^2\uparrow}$ to $\underline{3d}_{3z^2-r^2\downarrow}\underline{3d}_{x^2-y^2\downarrow}\underline{L}_{x^2-y^2\uparrow}$; see spectra (10) and (11) in Fig. 4(b). This is accompanied by a small but sudden increase in hole density due to the change in local symmetry. Note that close to the transition, the on-site energies of the x^2-y^2 orbital and

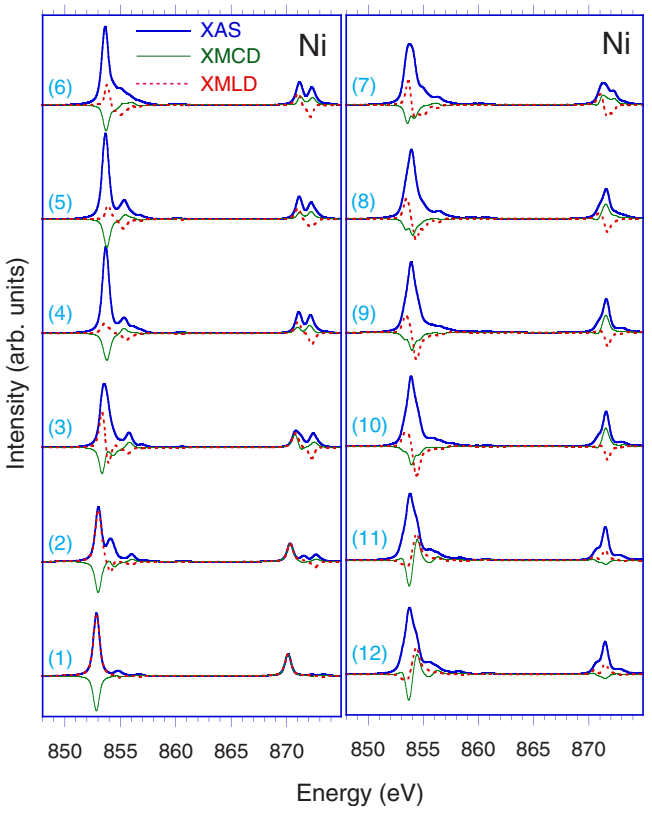

FIG. 5. (Color online) Ni L-edge x-ray absorption (blue), x-ray magnetic circular dichroism (thin green), and x-ray magnetic linear dichroism spectra (dotted red) for the values of the difference in work function given in Fig. 4.

the $3z^2-r^2$ orbital are comparable. This has a result that there is a little change in the isotropic x-ray absorption spectra; see spectra (10) and (11) in Fig. 5. However, the XMLD changes sign across the transition, reflecting the change in hole density from perpendicular to parallel to the interface. There is also a significant change in the x-ray magnetic circular dichroism (XMCD) (in the case where the Ni compound is paramagnetic or antiferromagnetic, the XMCD can be observed by applying a strong magnetic field, thereby canting the spins). After the change in local symmetry, charge fluctuations across the interface have strongly decreased and the magnetic coupling is very small, see Fig. 2(e), thereby strongly reducing the integrated intensity of XMCD. It is interesting to note that the transition can be manipulated by distortions; see the dotted lines in Fig. 4(b) where a Jahn-Teller distortion of 0.5 eV favors hole density in the Ni $3d_{x^2-y^2}$ orbital. This would allow for the manipulation of the transition by strain.

V. COBALT COMPOUNDS

Divalent cobalt is usually in a high-spin state $3d^3_{t_{2g}\uparrow}3d^2_{t_{2g}\downarrow}3d^2_{e_g\uparrow}$ (or $\underline{3d}_{t_{2g}\downarrow}\underline{3d}^2_{e_g\downarrow}$ in hole notation); see Fig. 6. The lowest electron-addition state is obtained by filling the t_{2g} hole. The lowest electron-removal state is much less obvious. This is for example exemplified by the decade-long discussion of the ground state of trivalent cobalt in $LaCoO_3$.

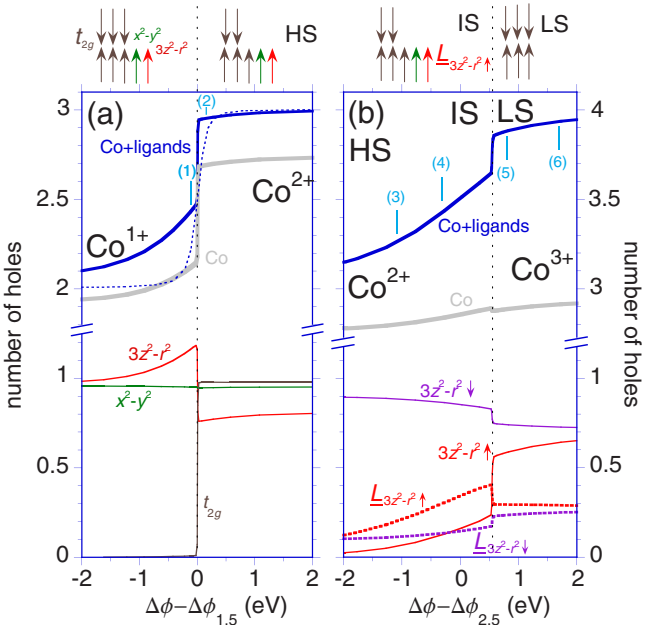

FIG. 6. (Color online) Hole densities on interfacial Co as a function of the difference in work function. (a) The hole densities in $3d_{x^2-y^2}$ (green), $3d_{3z^2-r^2}$ (red), the t_{2g} orbitals (brown), on Co total (gray), and on Co and the surrounding ligands (blue) on the CoO_6 cluster adjacent to the interface when the valency is changing from 1+ to 2+. The blue dotted line shows the total hole density on cobalt and the surrounding ligands when the reservoir couples to the t_{2g} states instead of the e_g states. The value of $\Delta\phi$ for $Co^{1.5+}$ has been subtracted. The numbers indicate the values for which x-ray absorption spectra have been calculated [see Fig. 5]. (b) The hole density in the $3d_{3z^2-r^2}$ orbital with spin up (↑, red solid curve) and spin down (↓, purple solid curve), in the ligand states with $3z^2-r^2$ symmetry with spin up (↑, red dotted curve) and spin down (↓, purple dotted curve), on Co total (gray), and on Co and the surrounding ligands (blue) when the valency is changing from 2+ to 3+ (the value of $\Delta\phi$ for $Co^{2.5+}$ has been subtracted). At the top are the dominant configurations of the Co ion for high (HS), intermediate (IS), and low (LS) spins.

At first, the consensus appeared that Co^{3+} ions are in a low-spin configuration[17,25] (t^6_{2g} and $^1A_1$ symmetry in O_h). This situation changed drastically when Korotin *et al.*[26] suggested that their LDA+U calculations indicated that $LaCoO_3$ could be intermediate spin $t^5_{2g}e^1$ ($S=1$). This debate on the nature of the ground state in $LaCoO_3$ is still ongoing.[27] This competition between different spin states will also be found when considering the local symmetries of cobalt ions at the interface.

Let us first consider the situation where the difference of the work function is changing such that electrons are transferred to the cobalt compound. We have to distinguish the situations where the material on the other side of the interface couples strongly to the t_{2g} or the e_g orbitals. The lowest state for Co^{1+} ($\underline{3d}^2_{e_g\downarrow}$) is comparable to Ni^{2+}. When the coupling to the interface is dominated by the t_{2g} orbitals, the transition is smooth, see the dotted line in Fig. 6(a), but with a narrow width in $\Delta\phi$ over which the change in electron density occurs due to the small hopping integral of the t_{2g}

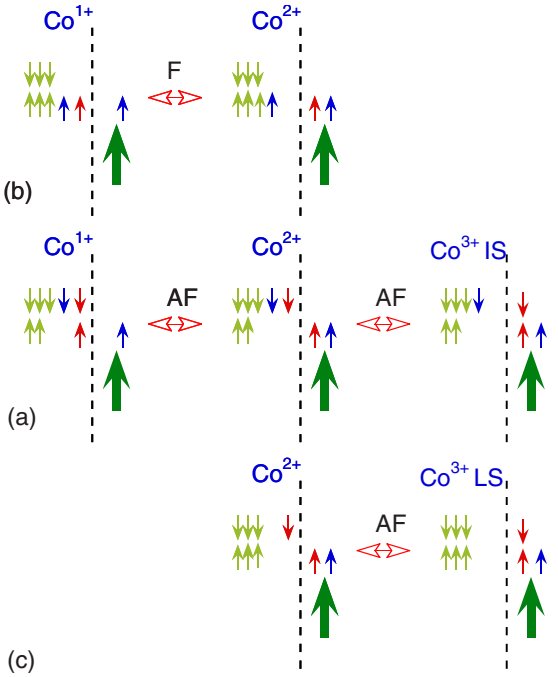

FIG. 7. (Color online) Schematic figure of the dominant charge fluctuations across the interface (indicated by the dashed line) for a cobalt system. The magnetic couplings are given for the situation where the "reservoir" is assumed to have the spin-up states occupied. The small red, blue, and green arrows indicate electrons in the x^2-y^2, $3z^2-r^2$, and t_{2g} orbitals, respectively. The large green arrow denotes a core spin leading to a spin polarization of the e_g electrons in the reservoir. (a) Antiferromagnetic charge fluctuations across the interface starting from a high-spin Co^{2+} configuration. Electron transfer to the cobalt leads to a high-lying multiplet and is suppressed. Electron removal from cobalt through the apical oxygen leads to an intermediate-spin state. These fluctuations correspond to points (2)–(4) in Fig. 6. (b) Charge fluctuations starting from the lowest Co^{1+} configuration lead to ferromagnetic couplings [point (1)]. (c) Charge fluctuations starting from a low-spin Co^{3+} configuration are weakly antiferromagnetic [points (5) and (6)].

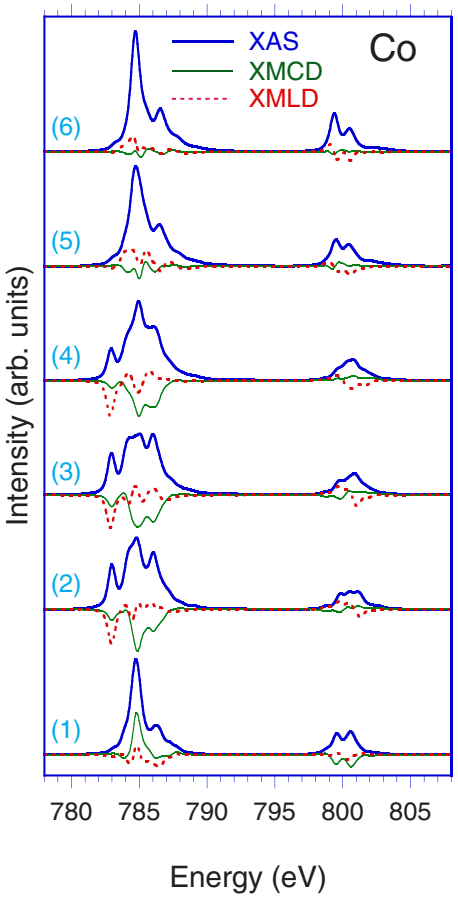

FIG. 8. (Color online) Co L-edge x-ray absorption (blue), x-ray magnetic circular dichroism (thin green), and x-ray magnetic linear dichroism spectra (dotted red) for the values of the difference in work function given in Fig. 6.

electrons. The situation is more interesting when the e_g states couple strongly to the interface. For $\Delta\phi-\Delta\phi_{1.5}>0$, point (2) in Fig. 6(a), electrons are transferred to Co through the covalent bond and the $3d_{3z^2-r^2}$ hole density is less than 1; see Figs. 6(a) and 9(a). Due to the $3d_{3z^2-r^2}$-L_{p_z}-$3d_{3z^2-r^2}$ covalent bond formation, a spin delocalizes over the interface causing an antiferromagnetic superexchange [see Fig. 7(a)]. When further transferring electrons to the Co or Fe (lowering $\Delta\phi$), there is a sudden change in electron densities. A transferred t_{2g} electron causes a reduction in the Co or Fe local moment. The covalent bond now starts working in the reverse direction. While for $\Delta\phi-\Delta\phi_{1.5}>0$ [point (1) in Fig. 6(a)] it increases the electron density on Co, for $\Delta\phi-\Delta\phi_{1.5}<0$ it decreases the electron density, giving a $3d_{3z^2-r^2}$ hole density larger than 1 [see Fig. 7(b)]. However, the covalent bond now causes a ferromagnetic double exchange interaction across the interface. Therefore, manipulation of the work-function difference can lead to a sign change in the magnetic coupling across the interface. This transition can be observed in the x-ray absorption spectra [see Fig. 8]. When cobalt is divalent, isotropic spectra resemble typical atomic calculations for Co^{2+} (Ref. 11); see spectra (2) and (3). When the electron density moves into the t_{2g} orbital, the spectral changes dramatically and resembles more closely that of divalent nickel. Note that there is also a change in sign of the XMCD. The spectra (2) and (3) show a strong dichroism at the absorption edge. This lowest feature is related to excitations into the empty t_{2g} state, which shows a strong linear dichroism. When all t_{2g} states are filled, the XMLD is strongly reduced [see spectrum (1)].

An interesting situation occurs when the valency of the cobalt adjacent to the interface is close to 3+. The majority of the additional holes go on the ligands orbitals around the cobalt site, see Fig. 6(b), and a $3d_{3z^2-r^2}$-L_{p_z}-$3d_{3z^2-r^2}$ covalent bond is formed. The hole in the covalent bond couples antiparallel to the cobalt moment. The dominant configuration $\underline{3d_{t_{2g}\downarrow}}\underline{3d^2_{e_g\downarrow}}\underline{L}_{3z^2-r^2\uparrow}$ is intermediate spin ($S=1$). The presence of the strongly covalent bond across the interface allows the stabilization of the intermediate-spin state up to a formal valency of $Co^{2.6+}$. However, a further increase in the valency is untenable. Although the intermediate-spin state is the lowest electron-removal state that has a finite spectral weight starting from a high-spin Co^{2+} ion,[13] it is, in fact, not the lowest electron-removal state. The lowest electron-removal

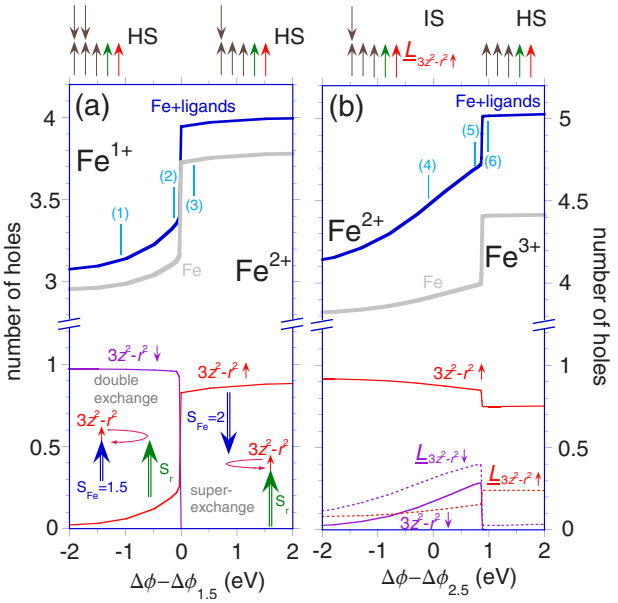

FIG. 9. (Color online) Hole densities on interfacial Fe as a function of the difference in work function. (a) The hole densities in $3d_{3z^2-r^2\uparrow}$ (red solid curve), $3d_{3z^2-r^2\downarrow}$ (purple solid curve), on Fe total (gray dotted), and on Fe and the surrounding ligands (blue) on the FeO_6 cluster adjacent to the interface when the valency is changing from 1+ to 2+. The value of $\Delta\phi$ for $Fe^{1.5+}$ has been subtracted. (b) Idem, but now the valency is changing from 2+ to 3+. In addition, the hole densities on $L_{3z^2-r^2\uparrow}$ (red dotted curve), $3d_{3z^2-r^2\downarrow}$ (purple dotted curve) are given. The value of $\Delta\phi$ for $Fe^{2.5+}$ has been subtracted.

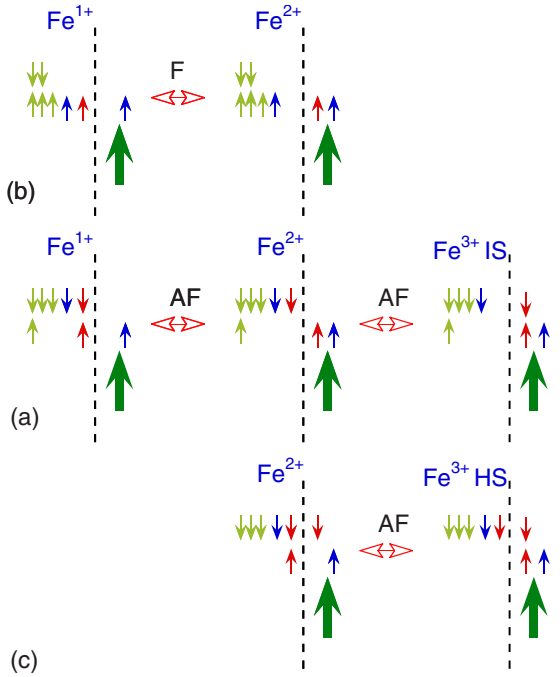

FIG. 10. (Color online) Equivalent to Fig. 7 but for iron. (a) Antiferromagnetic charge fluctuations across the interface starting from a high-spin Fe^{2+} configuration. Electron transfer to the iron leads to a high-lying multiplet and is suppressed. Electron removal from iron through the apical oxygen leads to an intermediate-spin state. This corresponds to points (3)–(5) in Fig. 9. (b) Charge fluctuations starting from the lowest Fe^{1+} configuration lead to ferromagnetic couplings [points (1) and (2)]. (c) Charge fluctuations starting from a low-spin Fe^{3+} configuration are weakly antiferromagnetic [point (6)].

state is low-spin $3d^6_{t_{2g}}$. This state has zero quasiparticle weight starting from a high-spin state, and one therefore has a sudden transition from intermediate to low spin accompanied by a jump in hole density; see spectra (4) and (5) in Fig. 6(b). After undergoing an intermediate-to-low-spin transition, the isotropic spectra (5) and (6) in Fig. 8 look remarkably similar to spectrum (1) as a result of the fact that $\underline{3d^2_{x^2-y^2}}\underline{3d^2_{3z^2-r^2}}$ is similar to the $\underline{3d_{x^2-y^2\uparrow}}\underline{3d_{3z^2-r^2\uparrow}}$ configuration. Obviously, there is a significant difference in the XMCD, which is close to zero for the low-spin systems; see spectra (5) and (6). For the XMLD, we again see the disappearance of the linear dichroic signal at the absorption edge related to the t_{2g} hole density.

VI. IRON COMPOUNDS

Possibilities for a change in sign of the magnetic coupling across the interface are also found for electron-doped iron; see Fig. 9(a). For a high-spin Fe^{2+} configuration, the hybridization across the interface is weak since it involves high-lying states due to the large core spin on iron [see Fig. 10(a)]. A further increase in the electron density on the iron atom adjacent to the interface results in the transfer of an electron to the t_{2g} states [see Fig. 10(b)]. This leads to a sudden increase (drop) in the electron (hole) density; see points (2) and (3) in Fig. 9(a). The electron transfer also leads to a change in the sign of the magnetic coupling. Before the transfer, electrons from the spin-up density of states in the reservoir couple to the empty DOS of the iron [see Fig. 10(a)]. After the charge transfer into the Fe t_{2g} states, the Fe spin-up DOS couples to the hole density in the spin-up DOS of the reservoir created by the transfer of electron across the interface. This transition also causes a significant change in the x-ray absorption spectral line shapes; see spectra (2) and (3) in Fig. 11.

Hole doping of iron leads to an intermediate-spin state of mainly $\underline{3d^2_{t_{2g}\downarrow}}\underline{3d^2_{e_g\downarrow}}\underline{L}_{3z^2-r^2\uparrow}$ with a spin moment $S=3/2$ [see Fig. 10(a)]. Again, this intermediate-spin state is strongly stabilized by the presence of a covalent bond, allowing an increase in formal valency of up to $Fe^{2.7+}$ [see Fig. 9(b)]. Unlike cobalt, intermediate-spin states are generally not discussed for iron compounds. Further removal of electrons from the iron causes a transition into an $S=5/2$ high-spin state [see Fig. 10(c)]. The spectral line shapes, see spectra (5) and (6) in Fig. 11, look very similar at first sight. However, there is a significant difference in the integrated intensities of the circular and linear dichroic spectra which are related to ground state expectation values of the orbital and the quadrupole moment, respectively, by the x-ray absorption sum rules.[28–30] Formally trivalent iron has the symmetry of a half-filled $3d$ shell ($^6A_1$) and has no orbital and quadrupolar moment. The integrated intensities of spectrum (6) are therefore close to zero. Formally divalent iron has an additional elec-

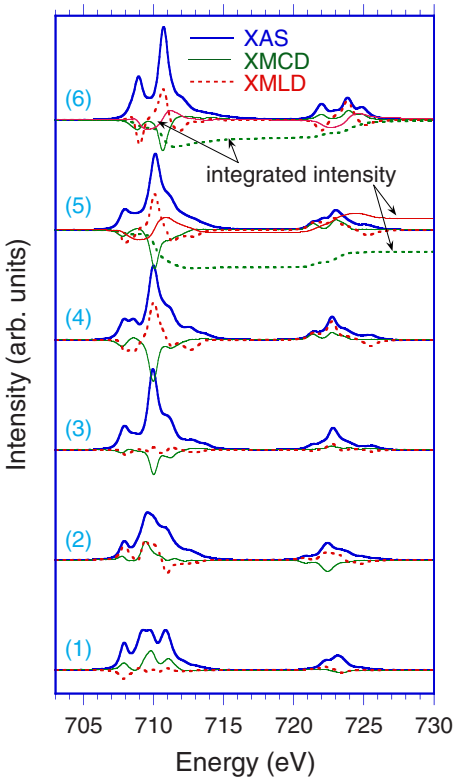

FIG. 11. (Color online) Fe L-edge x-ray absorption (blue), x-ray magnetic circular dichroism (thin green curve), and x-ray magnetic linear dichroism spectra (dotted red curve) for the values of the difference in work function given in Fig. 9. The integrated intensities of the circular and linear dichroism are also shown for the spectra indicated with (5) and (6).

tron in a t_{2g} orbital which does have a quadrupolar and, in the presence of spin-orbit coupling, a significant orbital moment; see the integrated intensities of spectrum (5) in Fig. 11.

VII. CONCLUSION

Summarizing, the local spin and orbital structure of transition-metal ions adjacent to an interface has been investigated. Transition-metal ions adjacent to the interface couple across the interface in one particular direction. Since the hybridization is often strongest for the e_g orbitals, this leads to the formation of a covalent bond involving the $3z^2-r^2$ orbitals. Electrons can now be exchanged between both sides of the interface while still benefitting from the stabilization energy of the covalent bond. However, a change in electron density through the apical oxygen often involves electron-removal and -addition states that are not the lowest in energy. This has a number of dramatic results. First, the transfer of electrons across the interface is often not a continuous process but involves sudden jumps in electron density. This is related to the presence of a "symmetry barrier." Although significant charge can be transferred across the interface through the covalent bond, at some point, the charge density will reorganize itself to involve the lowest bulk electron-removal states. Second, the strong covalent bonding across the interface creates unusual states that are not present in the bulk. Examples include significant hole density in $3d_{3z^2-r^2}$ orbitals in cuprates, which was demonstrated experimentally.[6] When electrons are removed from copper compounds, there is the possibility for Zhang-Rice triplet character at the interface. For both cobalt and iron oxides, intermediate-spin states can be stabilized at the surface. Third, interesting possibilities can occur when interfaces can be engineered to be sufficiently close to the orbital and spin reconstruction transitions that such switching between the different states can be achieved by an externally applied potential. Possibilities are orbital switches that can be made with a divalent copper or nickel compound interfaced with an electron acceptor or divalent copper with an electron donor.[6] When orbital reconstruction occurs, hole density is present in the $3d_{3z^2-r^2}$ orbital instead of $3d_{x^2-y^2}$. Further removal of electrons from the Cu/Ni side of the interface leads to a discrete transition, where the hole density switches to the $3d_{x^2-y^2}$ orbital. In addition, the strong magnetic coupling across the interface due to the orbital reconstruction[20] (ferromagnetic or antiferromagnetic following the usual Goodenough-Kanamori[17,19] rules) essentially disappears after the switching. Both cobalt and iron compounds offer the possibility of a sign change in the exchange interaction when interfaced with an electron donor. Increasing the electron density on the Co/Fe side of the interface leads to a change from a superexchange to a double exchange coupling across the interface.

This paper gives a qualitative description of different phenomena that can occur at the interfaces of transition-metal compounds to stimulate experimental work on interface phenomena using, e.g., x-ray absorption and dichroism. The effects are studied on one side of the interface with the other side treated as a reservoir that can extract or add electrons. This has a great advantage that trends can be studied across the transition-metal series. However, detailed studies are necessary to understand how the charge balance at the interface can be adjusted by varying the compounds, the doping level, and the strain. A detailed understanding of these phenomena offers the possibility of creating switching behavior with an externally applied potential, opening up the possibility of technological applications.

ACKNOWLEDGMENTS

John Freeland and Jak Chakhalian are acknowledged for useful discussions. This work was supported by the US Department of Energy (DOE) (Contract No. DE-FG02-03ER46097) and NIU's Institute for Nanoscience, Engineering, and Technology. Work at Argonne National Laboratory was supported by the US DOE, Office of Science, Office of Basic Energy Sciences under Contract No. DE-AC02-06CH11357.

*veenendaal@niu.edu

[1] S. Okamoto and A. J. Millis, Nature (London) **428**, 630 (2004).
[2] M. Huijben, G. Rijnders, D. H. A. Blank, S. Bals, S. van Aert, J. Verbeeck, G. van Tendeloo, A. Brinkman, and H. Hilgenkamp, Nature Mater. **5**, 556 (2006).
[3] N. Nakagawa, H. Y. Hwang, and D. A. Muller, Nature Mater. **5**, 204 (2006).
[4] S. Thiel, G. Hammerl, A. Schmehl, C. W. Schneider, and J. Mannhart, Science **313**, 1942 (2006).
[5] B. R. K. Nanda, S. Satpathy, and M. S. Springborg, Phys. Rev. Lett. **98**, 216804 (2007).
[6] J. Chakhalian, J. W. Freeland, H.-U. Habermeier, G. Cristiani, G. Khaliullin, M. van Veenendaal, and B. Keimer, Science **318**, 1114 (2007).
[7] F. C. Zhang and T. M. Rice, Phys. Rev. B **37**, 3759 (1988).
[8] R. Pentcheva and W. E. Pickett, Phys. Rev. Lett. **99**, 016802 (2007).
[9] N. Pavlenko, I. Elfimov, T. Kopp, and G. A. Sawatzky, Phys. Rev. B **75**, 140512(R) (2007).
[10] S. Yunoki, A. Moreo, E. Dagotto, S. Okamoto, S. S. Kancharla, and A. Fujimori, Phys. Rev. B **76**, 064532 (2007).
[11] F. M. F. de Groot, J. C. Fuggle, B. T. Thole, and G. A. Sawatzky, Phys. Rev. B **41**, 928 (1990).
[12] J. van Elp, H. Eskes, P. Kuiper, and G. A. Sawatzky, Phys. Rev. B **45**, 1612 (1992).
[13] J. van Elp, J. L. Wieland, H. Eskes, P. Kuiper, G. A. Sawatzky, F. M. F. de Groot, and T. S. Turner, Phys. Rev. B **44**, 6090 (1991).
[14] H. Eskes and G. A. Sawatzky, Phys. Rev. Lett. **61**, 1415 (1988).
[15] R. D. Cowan, *The Theory of Atomic Structure and Spectra* (University of California, Berkeley, 1981).
[16] M. A. van Veenendaal and G. A. Sawatzky, Phys. Rev. B **50**, 11326 (1994).
[17] J. B. Goodenough, *Magnetism and the Chemical Bond* (Interscience, New York, 1963).
[18] H. Eskes, L. H. Tjeng, and G. A. Sawatzky, Phys. Rev. B **41**, 288 (1990).
[19] J. Kanamori, J. Phys. Chem. Solids **10**, 87 (1959).
[20] J. Chakhalian, J. W. Freeland, G. Srajer, J. Strempfer, G. Khaliullin, J. C. Cezar, T. Chariton, R. Dalgliesh, C. Bernhard, G. Cristiani, H.-U. Habermeier, and B. Keimer, Nat. Phys. **2**, 244 (2006).
[21] G. A. Sawatzky and J. W. Allen, Phys. Rev. Lett. **53**, 2339 (1984).
[22] K. Terakura, A. R. Williams, T. Oguchi, and J. Kübler, Phys. Rev. Lett. **52**, 1830 (1984).
[23] A. Fujimori and F. Minami, Phys. Rev. B **30**, 957 (1984).
[24] See e.g., G. van der Laan, J. Zaanen, G. A. Sawatzky, R. Karnatak, and J.-M. Esteva, Phys. Rev. B **33**, 4253 (1986).
[25] P. M. Raccah and J. B. Goodenough, Phys. Rev. **155**, 932 (1967).
[26] M. A. Korotin, S. Y. Ezhov, I. V. Solovyev, V. I. Anisimov, D. I. Khomskii, and G. A. Sawatzky, Phys. Rev. B **54**, 5309 (1996).
[27] See e.g., M. W. Haverkort, Z. Hu, J. C. Cezar, T. Burnus, H. Hartmann, M. Reuther, C. Zobel, T. Lorenz, A. Tanaka, N. B. Brookes, H. H. Hsieh, H. J. Lin, C. T. Chen, and L. H. Tjeng, Phys. Rev. Lett. **97**, 176405 (2006), and reference therein.
[28] B. T. Thole, P. Carra, F. Sette, and G. van der Laan, Phys. Rev. Lett. **68**, 1943 (1992).
[29] P. Carra, B. T. Thole, M. Altarelli, and X. D. Wang, Phys. Rev. Lett. **70**, 694 (1993).
[30] P. Carra, H. König, B. T. Thole, and M. Altarelli, Physica B **192**, 182 (1993).